increasing current ratios and in fact decreases them in region 1 where these greater conductivity techniques are most useful. Comparison on the basis of the same electron temperature indicates that a nonequilibrium plasma will have slightly lower maximum current ratios than one in equilibrium. The former situation, however, may permit much higher temperature operation, far to the right in region 3 where maximum current ratios increase sharply. Similar calculations with helium indicate the same trends except that maximum current ratios are nearly one order of magnitude lower in region 1 whereas regions 2 and 3 begin at higher electron temperatures.

A one-dimensional coaxial device has been built to qualitatively check some of these theoretical predictions. Some preliminary experimental results described in Ref. 4 tend to substantiate them, although current ratios obtained up to this time have not been as large as expected.

References

[1] Cowling, T. C., *Magnetohydrodynamics*, Interscience, New York, 1957.

[2] Demetriades, S. T. and Argyropoulos, G. S., "Ohm's Law in Multicomponent Nonisothermal Plasmas with Temperature and Pressure Gradients," *The Physics of Fluids*, Vol. 9, 1966, pp. 2136–2149.

[3] Henry, R. P., "Lorentz Force Maximization in Continuous Flow Hall Current Plasma Accelerators," *AIAA Journal*, Vol. 4, No. 1, Jan. 1966, pp. 165–166.

[4] Henry, R. P. and Scott, D. S., "Ion-Slip Limitations on Currents in Hall-Effect Plasma Accelerators," UTME-TP 6805, June 1968, Department of Mechanical Engineering, University of Toronto, Canada.

A Multiple Time Scaling Analysis of Re-Entry Roll Dynamics

Ali Hasan Nayfeh*

Aerotherm Corporation, Mountain View, Calif.

1. Introduction

THE rigid-body motion of a body entering the atmosphere depends upon many factors, such as the initial conditions, the mass and mass distribution, the external geometry, and the heat shield material. Since, in practice, vehicles have varying degrees of asymmetries, there is a coupling of the pitch and yaw degrees of freedom with the roll degree of freedom. The resultant heating and ablation will be asymmetric and new asymmetries will be induced.

Most theories for rolling symmetrical missiles have made use of the basic ballistic analysis of Fowler et al.,[3] Nicolaides,[9] and Charters[1] obtained theories for rolling missiles having slight configurational asymmetries using nonrolling coordinate systems. Nelson[8] obtained a theory for slightly asymmetrical missiles using a body-fixed coordinate system. However, all of these theories, like that of Fowler, are linear and assume constant roll rate and freestream conditions. Coakley,[2] on the other hand, obtained a solution for the time variations of the angle of attack of rolling symmetrical missiles using the WKBJ method.[4] In Ref. 2, the roll rate is decoupled from the other degrees of freedom but the time variation of the freestream conditions is accounted for.

In this Note, approximate solutions are obtained for the roll rate and angle of attack for missiles with slight center of gravity and aerodynamic trim asymmetries using the method of multiple time scales.[5,6] The time variation of the freestream conditions as well as the coupling of the roll rate with the other degrees of freedom are taken into account. The analysis is based upon the observation that there are at least two time scales: a slow time characterizing the variation of the dynamic pressure and a fast time characterizing the angle-of-attack oscillations.

It is assumed that gravity forces are negligible, and the aerodynamic forces and moments are linear. Velocities, atmospheric density, and time are made dimensionless using the entry velocity u_e, sea-level density ρ_s, and characteristic time $T = [2I/\rho_s u_e^2 Ad]^{1/2}$, where I is the transverse moment of inertia and d and A are the body diameter and cross-sectional area, respectively.

A right-handed orthogonal body-fixed coordinate system is introduced such that the x axis is the longitudinal axis, the y axis is the horizontal transverse axis, and the z axis is orthogonal to the x and y axes. The velocity components along these axes are denoted by u, v, and w, and the angular velocities about these axes are denoted by p, q, and r, respectively. The six-degree-of-freedom equations of motion can be transformed into[7]

$$\dot{u} + qw - rv = -\epsilon\rho V^2 \tag{1}$$

$$\dot{p} = \rho V^2[\epsilon C_{l0} + C_{N\alpha}\alpha c/d + \epsilon\nu C_{lp}p/V]/(1 - \gamma) \tag{2}$$

$$\ddot{\delta} + [ip(1 + \gamma) + \dot{u}/u + \epsilon Q - \epsilon D]\dot{\delta} + [i\dot{p} + \gamma(p_c^2 - p^2) + ip(\gamma\dot{u}/u - \epsilon D - \epsilon M + \epsilon\gamma Q/u)]\delta - \gamma\ddot{\delta}_t + 0(\epsilon^2\delta) = 0 \tag{3}$$

where the complex angle of attack $\delta = \beta + i\alpha$, $p_c^2 = -\rho V^2 C_{m\alpha}/\gamma$, $\gamma = 1 - I_x/I$, $Q = \rho V^2 C_{N\alpha}/C_D$, $D = \rho V\nu(C_{m\dot{\alpha}} + C_{mq})$, $M = \rho V\nu C_{mp\alpha}$, $\nu = md^2/2IC_D$, $\epsilon = [\rho_s I/2Ad]^{1/2}/B$, and $B = m/C_D A$. Here, C_D is the drag coefficient, C_{lp} is the roll damping coefficient, C_{l0} is the pure roll torque coefficient, $C_{m\alpha}$ and $C_{mp\alpha}$ are the pitching and Magnus moment coefficients, C_{mq} and $C_{m\dot{\alpha}}$ are the pitch or yaw damping derivatives, $C_{N\alpha}$ is the normal force derivative, I_x is the axial moment of inertia, m is the vehicle mass, and V is the absolute velocity.

2. Analysis

Actual flight test data and six-degree-of-freedom numerical calculations show that there are at least two time scales: a slow time characterizing the variation of velocity and a fast time characterizing the angle-of-attack oscillations. This suggests the applicability of the method of multiple scales[5,6] to determine an asymptotic solution for Eqs. (1–3) for small ϵ.

Introduce a slow time $\tau = \epsilon t$ and a fast time $\eta = g(\tau)/\epsilon$ where $g(\tau)$ is an unknown function that will be determined in the course of analysis. Assume that $\delta_t = \epsilon\delta_t$, and u, p, and δ possess the following expansions:

$$u(t) = u_0(\tau,\eta) + \epsilon u_1(\tau,\eta) + \ldots \tag{4}$$

$$p(t) = p_0(\tau,\eta) + \epsilon p_1(\tau,\eta) + \ldots \tag{5}$$

$$\delta(t) = \epsilon\delta_1(\tau,\eta) + \epsilon^2\delta_2(\tau,\eta) + \ldots \tag{6}$$

Substitute these expansions into Eqs. (1–3) and equate coefficients of equal powers of ϵ. The solutions of the resulting equations contain arbitrary functions of τ. These functions as well as $g(\tau)$ will be determined by requiring that Eqs. (4–6) be uniformly valid expansions; i.e., the second terms are small corrections to the first terms. Thus, it is required that u_1/u_0, p_1/p_0, and $\delta_2/\delta_1 < \infty$ for all η and τ.

The zeroth-order equations lead to

$$u_0 = u_0(\tau) \text{ and } p_0 = p_0(\tau) \tag{7}$$

Therefore, Q, M, D, p_c, and C_{l0} are functions of the slow time

Received December 10, 1968; revision received June 9, 1969.

* Manager, Mathematical Physics Department. Member AIAA.

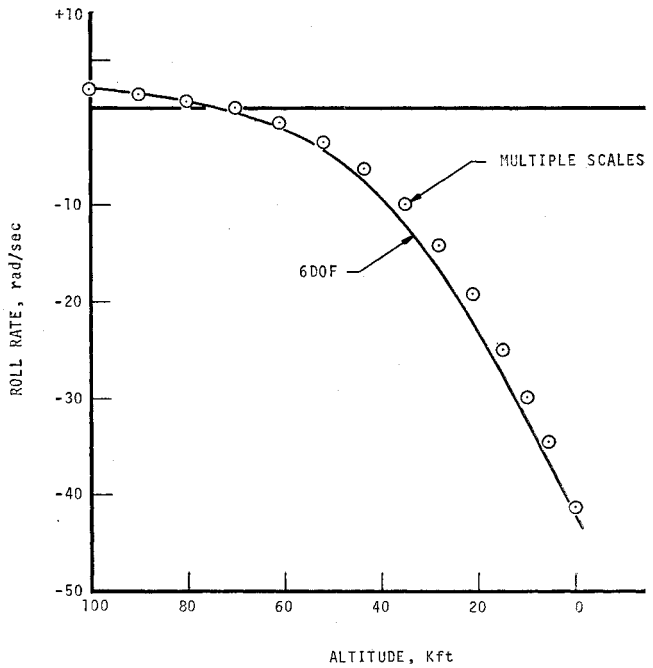

Fig. 1 Comparison of the roll rate obtained from the multiple time scaling analysis with that obtained from 6-degree-of-freedom computation ($p_0 = 2$ rad/sec and $u_e =$ 20,000 fps at 100 kft, $m = 95$ lb, $B = 1475$ psf, $A = 0.92$ ft^2, $D = 1.08$ ft, $C_{m\alpha} = -0.006$/deg, $C_{N\alpha} = 0.045$/deg, $\alpha_t = 0.15°$, $\beta_t = 0$, and $c = 0.03$ in.).

to first order. Consequently, the solution for δ_1 is

$$\delta_1 = F(\tau) + A_1(\tau)\exp[ih_1(\tau)\eta] + A_2(\tau)\exp[ih_2(\tau)\eta] \quad (8)$$

where

$$F(\tau) = \delta_t/(1-k^2),\ k = p_3/p_c$$

$$g'h_{1,2} = -(1+\gamma)p_0/2 \pm \omega,\ \omega^2 = [(1-\gamma)p_0/2]^2 + \gamma p_c^2$$

$$A_m(\tau) = a_m(\tau)\exp[i\phi_m(\tau)],\ m = 1,2$$

with a_m and ϕ_m real-valued functions.

Using Eqs. (7) and (8) and requiring p_1/p_0 be bounded for all η yield[7]

$$\frac{dp_0}{d\tau} = \xi = \rho_0 u_0\left[C_{l0} + \frac{c}{d}C_{N\alpha}\alpha_t\Big/(1-k^2)\right] \quad (9)$$

$$p_1 = b\left[\frac{a_1}{h_1}\cos\mu_1 + \frac{a_2}{h_2}\cos\mu_2\right]\Big/g' \quad (10)$$

with $b = \rho_0 u_0^2 c C_{N\alpha}/d$, $\mu_m = h_m\eta + \phi_m$. Imposing the condition that u_1/u_0 be bounded for all η gives[7]

$$du_0/d\tau = -\rho_0 u_0^2 \quad (11)$$

To solve for u_0, the variation of ρ_0 with time is needed. For an exponentially varying atmosphere,

$$d\rho_0/d\tau = (2B/\rho_s H)\rho_0 u_0 \sin\theta \quad (12)$$

where θ is the trajectory angle and H is the atmospheric scale height.

The equation for δ_2 becomes[7]

$$L(\delta_2) = -i\sum_{m=1}^{2}\left\{R_m\exp(i\mu_m) - b(\beta_t + i\alpha_t)a_m\left[\sin\mu_m - \frac{2\gamma p_0}{g'h_m}\cos\mu_m\right]\right\} + \text{terms}$$

$$\{\text{independent of } \eta, \text{ proportional to } \exp[\pm\mu_1 \pm\mu_2]\} \quad (13a)$$

where

$$L = g'^2\partial^2/\partial\eta^2 + ip_0 g'(1+\gamma)\partial/\partial\eta + \gamma(p_c^2 - p_0^2) \quad (13b)$$

$$R_m = [g'' + eg']a_m h_m + [2g'h_m + (1+\gamma)p_0]\times [a'_m + ia_m\phi'_m + ia_m h'_m\eta] + 2g'a_m h'_m + fa_m \quad (14)$$

$$e = -2\lambda + u'_0/u_0,\ \lambda = \tfrac{1}{2}(D_0 - Q_0/u_0) \quad (15)$$

$$f = \xi + p_0[\gamma u'_0/u_0 - D_0 - M_0 + \gamma Q_0/u_0] \quad (16)$$

with Q_0, D_0, and M_0 the first-order terms in Q, D, and M. The particular solution of Eq. (13) contains terms proportional to $[\eta^2,\eta][\cos\mu_m, \sin\mu_m]$, which make δ_2/δ_1 unbounded as $\eta \to \infty$. These terms will be eliminated if

$$R_m + \tfrac{1}{2}s(\beta_t + i\alpha_t)a_m = 0 \quad (17)$$

where $s = \frac{1}{2}b(1 + 2\gamma p_0/g')/(1-k^2)$. Since Eq. (17) is valid for all η,

$$h'_m = 0 \quad (18)$$

Hence, $h_m = $ const, which can be taken to be unity without loss of generality. Then, there are two possible values for g, which are given by

$$g'_{1,2} = -(1+\gamma)p_0/2 \pm \omega \quad (19)$$

Using Eq. (18), separating real and imaginary parts in Eq. (19), and solving the resulting equations lead to

$$\phi'_m = \pm s\beta_t/2\omega \quad (20)$$

$$a_m = \frac{\tilde{a}_m}{(u_0\omega)^{1/2}}\exp\left[\int_0^\tau(\lambda + \Delta\lambda_m)d\tau\right] \quad (21)$$

where a_m is an arbitrary constant and

$$\Delta\lambda_m = \pm\{[(1+\gamma)/2](p_0 e + \xi) - f - s\alpha_t\}/2\omega \quad (22)$$

3. Concluding Remarks

Equation (21) shows that the angle-of-attack convergence depends on the square root of the missile velocity. The smaller the velocity, the larger is the angle of attack. Equations (9, 15, 16, and 22) show that the angle-of-attack convergence depends on the roll acceleration, the vehicle deceleration, and the trim angles of attack in addition to the damping and Magnus forces.

Figure 1 shows good agreement between the roll rate calculated from Eqs. (9) and (10) and that obtained from a six-degree-of-freedom computation. The analysis needs to be applied to other missile parameters and compared with actual flight test data and six-degree-of-freedom numerical computation.

References

[1] Charters, A. C., "The Linearized Equations of Motions Underlying the Dynamic Stability of Aircraft, Spinning Projectiles, and Symmetrical Missiles," TN 3350, 1955, NACA.

[2] Coakley, T. J., "Dynamic Stability of Symmetric Spinning Missiles," *Journal of Spacecraft and Rockets*, Vol. 5, No. 10, Oct. 1968, pp. 1231–1232.

[3] Fowler, R. H. et al., "The Aerodynamics of a Spinning Shell," *Philosophical Transactions of the Royal Society of London, Series A*, Vol. 221, 1920, pp. 295–387.

[4] Morse, P. M. and Feshbach, H., *Methods of Theoretical Physics*, Vol. II, McGraw-Hill, New York, 1953.

[5] Nayfeh, A. H., "An Expansion Method for Treating Singular Perturbation Problems," *Journal of Mathematical Physics*, Vol. 6, No. 12, 1965, pp. 1946–1951.

[6] Nayfeh, A. H., "Forced Oscillations of the van der Pol Oscillator with Delayed Amplitude Limiting," *IEEE Transactions on Circuit Theory*, Vol. CT-15, No. 3, 1968, pp. 192–200.

[7] Nayfeh, A. H., "A Multiple Time Scaling Analysis of Reentry Roll Dynamics," *Transactions of the 3rd Technical Work-*

shop on Dynamic Stability Problems, Vol. II, NASA Ames Research Center, Moffett Field, Calif., Nov. 1968.

[8] Nelson, R. L., "The Motions of Rolling Symmetrical Missiles Referred to a Body-Axis System," TN 3737, 1956, NACA.

[9] Nicolaides, J. D., "On the Free Flight Motion of Missiles Having Slight Configurational Asymmetries," Rept. 858, June 1953, Ballistic Research Labs., Aberdeen Proving Ground, Md.

View Factor from Conical Surface by Contour Integration

J. B. URQUHART*
The Boeing Company, Huntsville, Ala.

Introduction

THE prediction of radiative heat transfer from the engine exhaust plume to the stage is necessary to evaluate thermal protection requirements. Therefore, the radiation view factor between the plume and the stage must be evaluated to determine the radiant heat rates. The normal approach to this problem is to assume that the exhaust plume behaves as a radiating cone; thus the problem is reduced to determining the view factor between a conical surface and a differential area on the stage. Using this approach, Morizumi[1] and Bobco[2] attempted to evaluate the view factor from a differential area to a cone. Morizumi used the Nusselt double-projection method. His analysis has the disadvantage of determining the view factor to a conical surface that is truncated by the differential-area line of sight instead of by a plane perpendicular to the cone axis. Bobco attempted to develop an expression for the view factor by integrating the general equation for view factors;

$$F_{dA_1-A_2} = \int\int_{A_2} \frac{\cos\theta_1 \cos\theta_2}{\pi r^2 dA_2} \tag{1}$$

where θ_1, θ_2, and r are indicated in Fig. 1. He successfully integrated Eq. (1) once but was then forced to integrate the resulting expression numerically.

Analysis

An analysis is developed here that will yield the view factor from a differential area to a cone. By applying Stokes theorem[3] to Eq. (1) the view-factor equation is reduced to contour integrals. For the configuration of interest (Fig. 1) the differential-area normal is parallel to the cone axis. The view factor for this configuration can therefore be represented

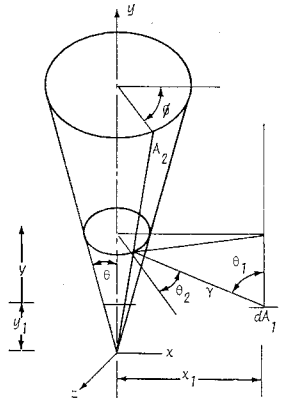

Fig. 1 View factor from differential area to cone.

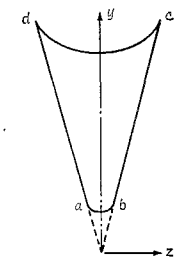

Fig. 2 Contour lines.

as a single contour integral

$$F_{dA_1-A_2} = \oint_{c_2} \frac{(x - x_1)dz - zdx}{2\pi r^2} \tag{2}$$

This contour integral is integrated around the path that is the limit of sight on the cone from the differential area. The contour path is shown in Fig. 2.

To integrate Eq. (2), x and z are written in polar form using the cone radius R and the angle ϕ measured from the x axis in the $x - z$ plane. The cone radius is

$$R = y \tan\theta \tag{3}$$

where θ is the half angle of the cone. Employing symmetry and expanding Eq. (2) into regular integrals yields

$$F_{dA_1-A_2} = \int_0^{-\phi_0} \frac{(y_1^2 \tan^2\theta - x_1 y_1 \tan\theta \cos\phi)d\phi}{\pi r^2} + \int_{y_1}^{\bar{y}} \frac{x_1 \tan\theta \sin\phi_0 dy}{\pi r^2} + \int_{-\phi_0}^{0} \frac{(\bar{y}^2 \tan^2\theta - x_1\bar{y} \tan\theta \cos\phi)d\phi}{\pi r^2} \tag{4}$$

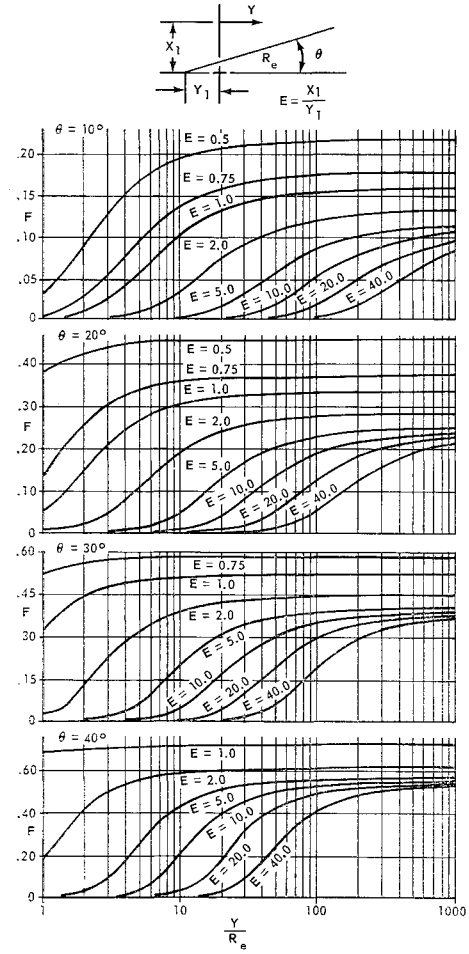

Fig. 3 View factor vs distance along cone axis for various *E*'s and θ's.

Received May 22, 1969.

* Associate Research Engineer.